iScience

CellPress
OPEN ACCESS

Article

The role of m6A modification in the risk prediction and Notch1 pathway of Alzheimer's disease

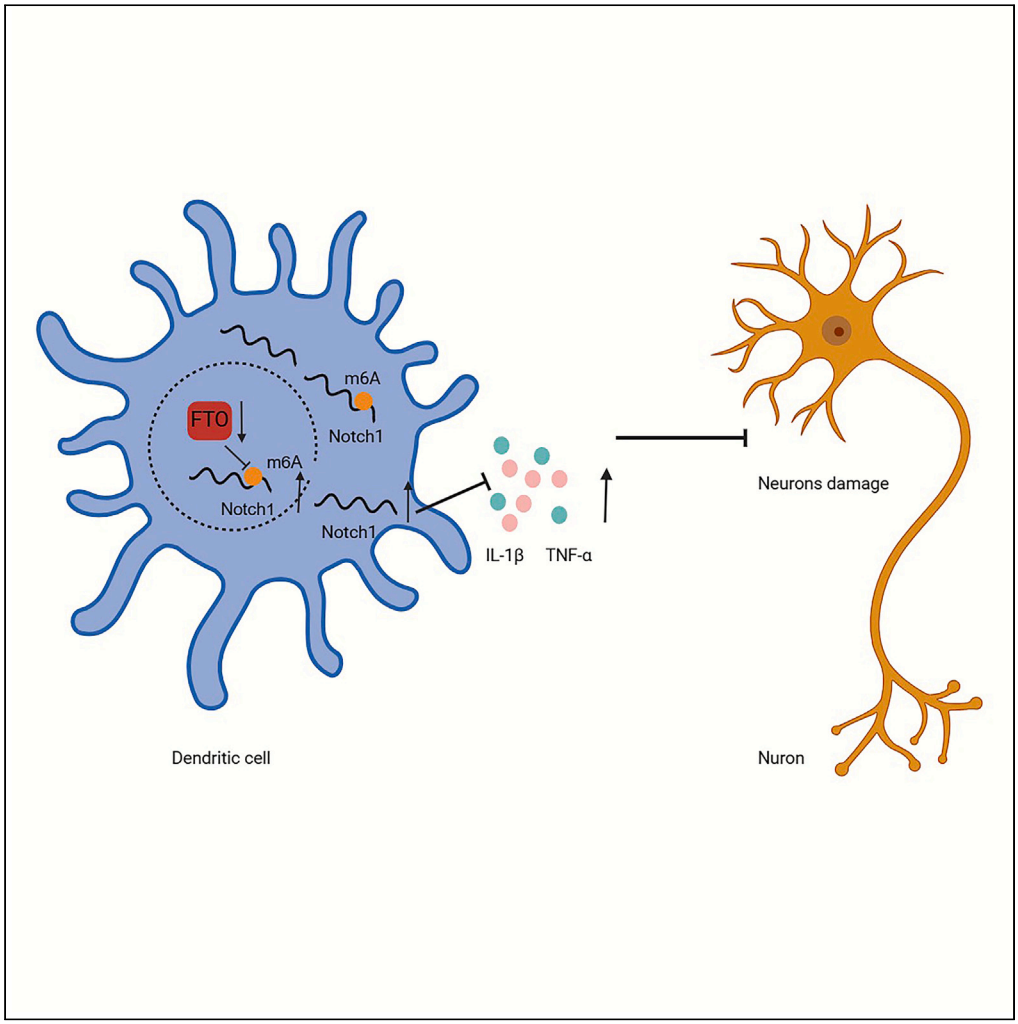

Yingdan Qiao, Yingna Mei, Minqi Xia, Deng Luo, Ling Gao

ling.gao@whu.edu.cn

Highlights

The nomogram model predicts AD risk, with FTO being the most important regulator

FTO downregulation in dendritic cells triggers AD inflammation via Notch1-Hes1 pathway

FTO negatively modulates the Notch1 pathway through Notch1 m6A modification

Upregulating the expression of Notch1 leads to an increase of TNF-α and IL-1β

Qiao et al., iScience 27, 110235
July 19, 2024
https://doi.org/10.1016/j.isci.2024.110235

iScience

CellPress
OPEN ACCESS

Article

The role of m6A modification in the risk prediction and Notch1 pathway of Alzheimer's disease

Yingdan Qiao,[1,2] Yingna Mei,[1,2] Minqi Xia,[1] Deng Luo,[1] and Ling Gao[1,3,*]

SUMMARY

N6-methyladenosine (m6A) methylation and abnormal immune responses are implicated in neurodegenerative diseases, yet their relationship in Alzheimer's disease (AD) remains unclear. We obtained AD datasets from GEO databases and used AD mouse and cell models, observing abnormal expression of m6A genes in the AD group, alongside disruptions in the immune microenvironment. Key m6A genes (YTHDF2, LRPPRC, and FTO) selected by machine learning were associated with the Notch pathway, with FTO and Notch1 displaying the strongest correlation. Specifically, FTO expression decreased and m6A methylation of Notch1 increased in AD mouse and cell models. We further silenced FTO expression in HT22 cells, resulting in upregulation of the Notch1 signaling pathway. Additionally, increased Notch1 expression in dendritic cells heightened inflammatory cytokine secretion *in vitro*. These results suggest that reduced FTO expression may contribute to the pathogenesis of AD by activating the Notch1 pathway to interfere with the immune response.

INTRODUCTION

Alzheimer's disease (AD) is an age-related progressive neurodegenerative disease, which is characterized by cognitive impairment and various neuropsychiatric symptoms.[1] The pathogenesis of AD is complex, involving a variety of susceptibility genes and environmental factors. Given the stimulating interaction between genetics and the external environment, epigenetics may become a new direction for the treatment of AD.[2,3] At present, much evidence has shown that AD patients have significant epigenetic changes in the brain, such as low expression of DNA methylation, histone acetylation, and so on.[4,5]

As a new kind of epigenetic transcriptome modification, RNA modification mediates the production and degradation of RNA, affects gene expression patterns, and regulates biological functions. m6A, the most common RNA modification in eukaryotes, plays a significant role in the degradation, translation, splicing, localization, and folding of RNA.[6–8] m6A modification mainly involves methyltransferase (writers, such as METTL3 and METTL14),[9] demethylase (eraser, such as FTO and ALKBH5)[10,11] and binding protein (reader, such as HNRNPA2B1, LRPPRC, and YTHDF2).[12–14] Previous research have shown that m6A genes were highly expressed in the brain and exerted great effects in brain development, neural stem cell differentiation, and learning and memory function.[15–17] Abnormal regulation of m6A might lead to neurodegenerative diseases.[18]

m6A can regulate the development, differentiation, activation, migration, and polarization of immune cells, thereby modulating both pro-inflammatory and anti-inflammatory responses.[19] For example, YTHDF2-deficient mice showed increased expression of inflammatory transcription, activating chronic inflammation.[20] Besides, recent studies have found that an over-activated immune response may exacerbate the progression of AD.[21–23] However, whether m6A genes are involved in pathological process of AD via its regulatory effects on immune microenvironment in the brain remains unclear. Machine learning has been explored for disease diagnosis, including the biological and diagnostic aspects of AD.[24,25] Machine learning algorithms such as random forest (RF) and support vector machine (SVM) are widely employed to screen for m6A-related genes associated with diseases.[26,27] Therefore, based on the AD database in GEO and AD mouse and cell models, we explored the expression pattern and risk assessment role of m6A regulators in AD, and further explored the specific mechanism of key m6A genes (FTO etc.) on the progression of AD in relation to immune microenvironments (Figure 1).

RESULTS

Expression patterns of m6A regulators in AD and NC samples

Twenty three m6A genes were mapped their positions on chromosomes by "RCircos" package[28] (Figure 2A). Differential expression analysis was applied to explore the expression patterns of 23 m6A genes in AD group and normal group. The expression of METTL14, ZC3H13,

[1]Department of Endocrinology & Metabolism, Renmin Hospital of Wuhan University, Wuhan, P.R. China
[2]These authors contributed equally
[3]Lead contact
*Correspondence: ling.gao@whu.edu.cn
https://doi.org/10.1016/j.isci.2024.110235

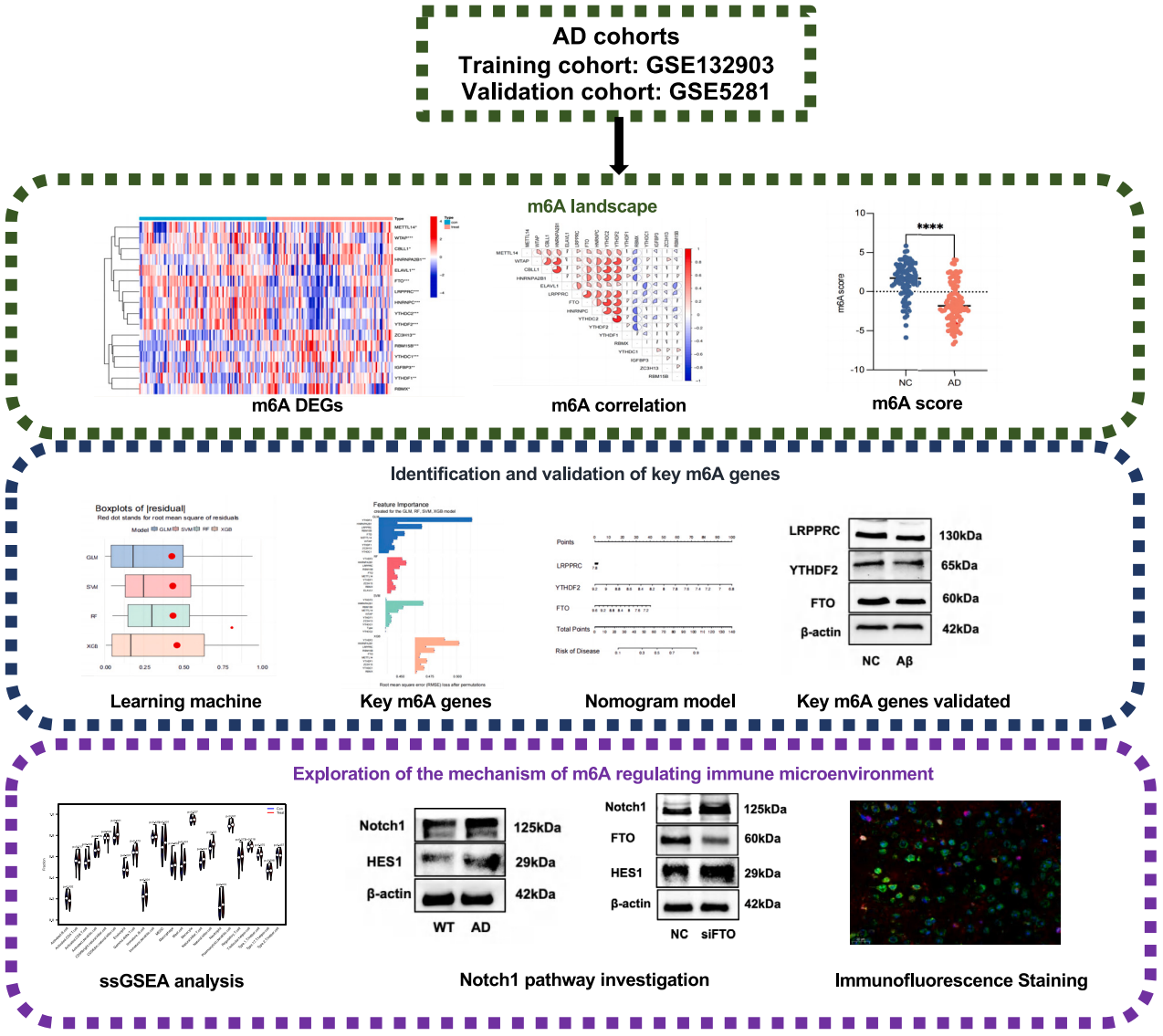

Figure 1. Over view of the study design

Based on GEO database, we explored the m6A landscape in AD samples. Next, we investigated and verified the predictive significance of key m6A genes for AD. Based on three key m6A genes, we explored the mechanism of m6A regulating immune microenvironment.

RBM15B, YTHDC1, YTHDF1, HNRNP2B1, IGFBP3, and RBMX was up-regulated in the AD group compared to NC group (Figure 2D), while the expression of WTAP, CBLL1, YTHDC2, YTHDF2, HNRNPC, LRPPRC, ELAVL1, and FTO was decreased in the AD group (Figure 2D). The correlation among sixteen differentially expressed m6A regulators indicated that these regulators were closely correlated with each other (Figures 2E and 2F), among which YTHDF2 and YTHDC2 had the highest positive correlation (correlation coefficient 0.77, Figure 2G), while YTHDF2 negatively associated with RBMX (correlation coefficient −0.58, Figure 2H). Based on the expression of sixteen differential expressed m6A regulators, we applied principal-component analysis (PCA) to calculate the m6A score of each sample. The m6A score in AD samples was significantly lower than normal samples (Figure 2B, $p < 0.0001$). We further examined the m6A RNA methylation in hippocampus of AD mice, and the results showed a significant increase compared to WT mice (Figure 2C, $p < 0.001$). This suggested that the abnormal expression of m6A regulators, which impacted the m6A methylation of diverse genes, may contribute to the progression of AD.

The identification of key m6A genes

In order to identify the key m6A genes in AD, we applied the machine learning algorithms to establish the generalized linear model (GLM), RF, XGboost (XGB), and SVM models. Compared with SVM, RV, and XGB, GLM has a smaller residual distribution (Figures 3A and 3B).

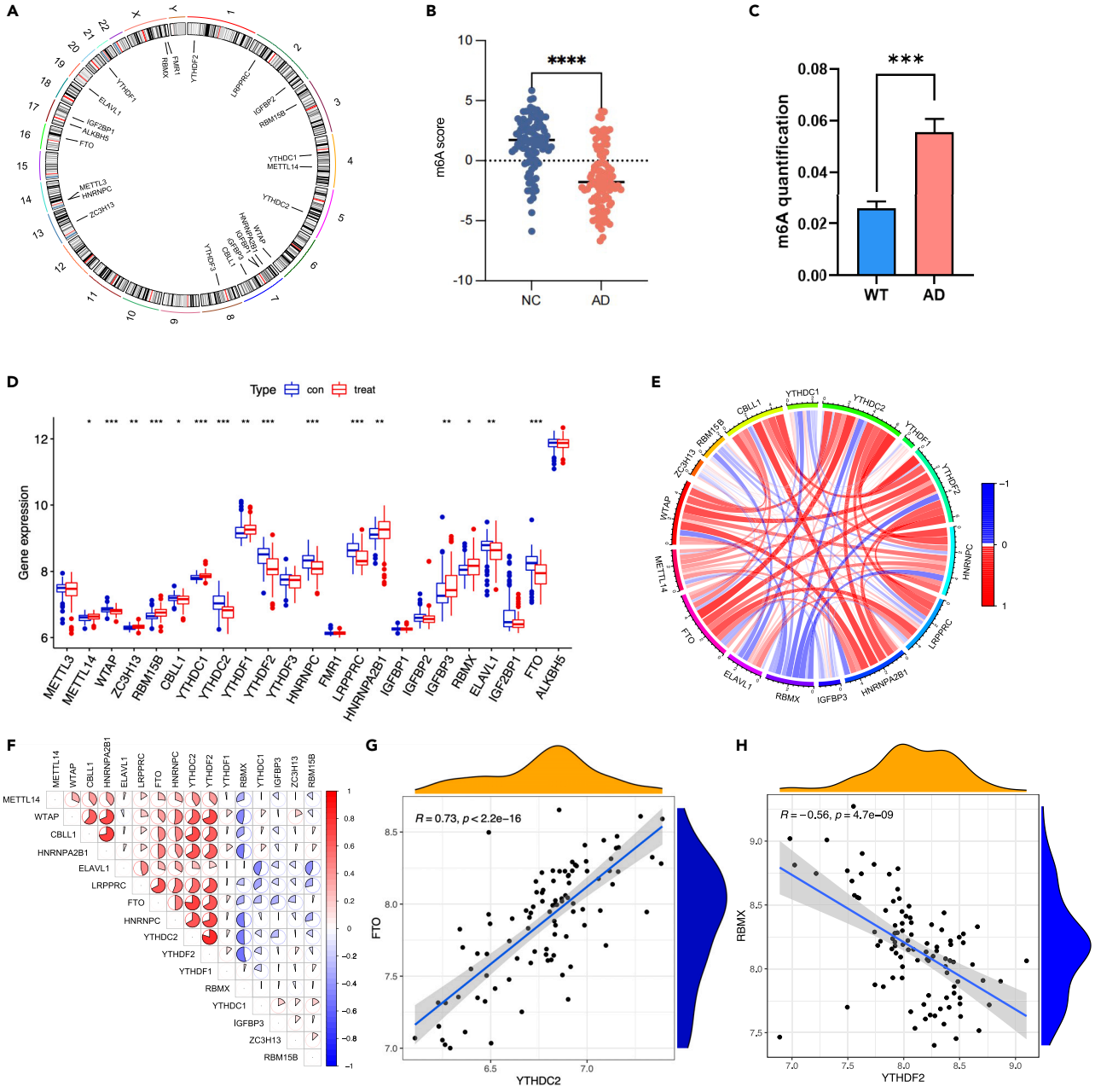

Figure 2. Expression patterns of m6A regulators in AD and NC samples

(A) The position of 23 m6A regulators in the chromosome.

(B) The scores of m6A regulators between AD samples and normal samples.

(C) The m6A RNA methylation in hippocampus of AD group and WT group. Data were represented as mean ± SEM (n=3).

(D) The expression of 23 m6A regulators in AD samples and control samples exhibited in the boxplot.

(E and F) The correlation among 16 m6A regulators in AD samples via spearman correlation analysis.

(G and H) Scatterplots were used to show the highest correlation among m6A regulators: YTHDF2 and YTHDC2 (positive correlation), YTHDF2 and RBMX (negative correlation). *$p < 0.05$, **$p < 0.01$, ***$p < 0.001$, ****$p < 0.0001$ was considered statistically significant.

Moreover, according to receiver operating characteristic (ROC) curve, GLM has larger area under the curve and higher prediction accuracy than other machine learning algorithms (Figure 3C). Based on the aforementioned results, we choose GLM as the optimal model. The first three m6A genes (YTHDF2, LRPPRC, and FTO) were selected based on importance ranking for the subsequent diagnostic prediction model (Figure 3D).

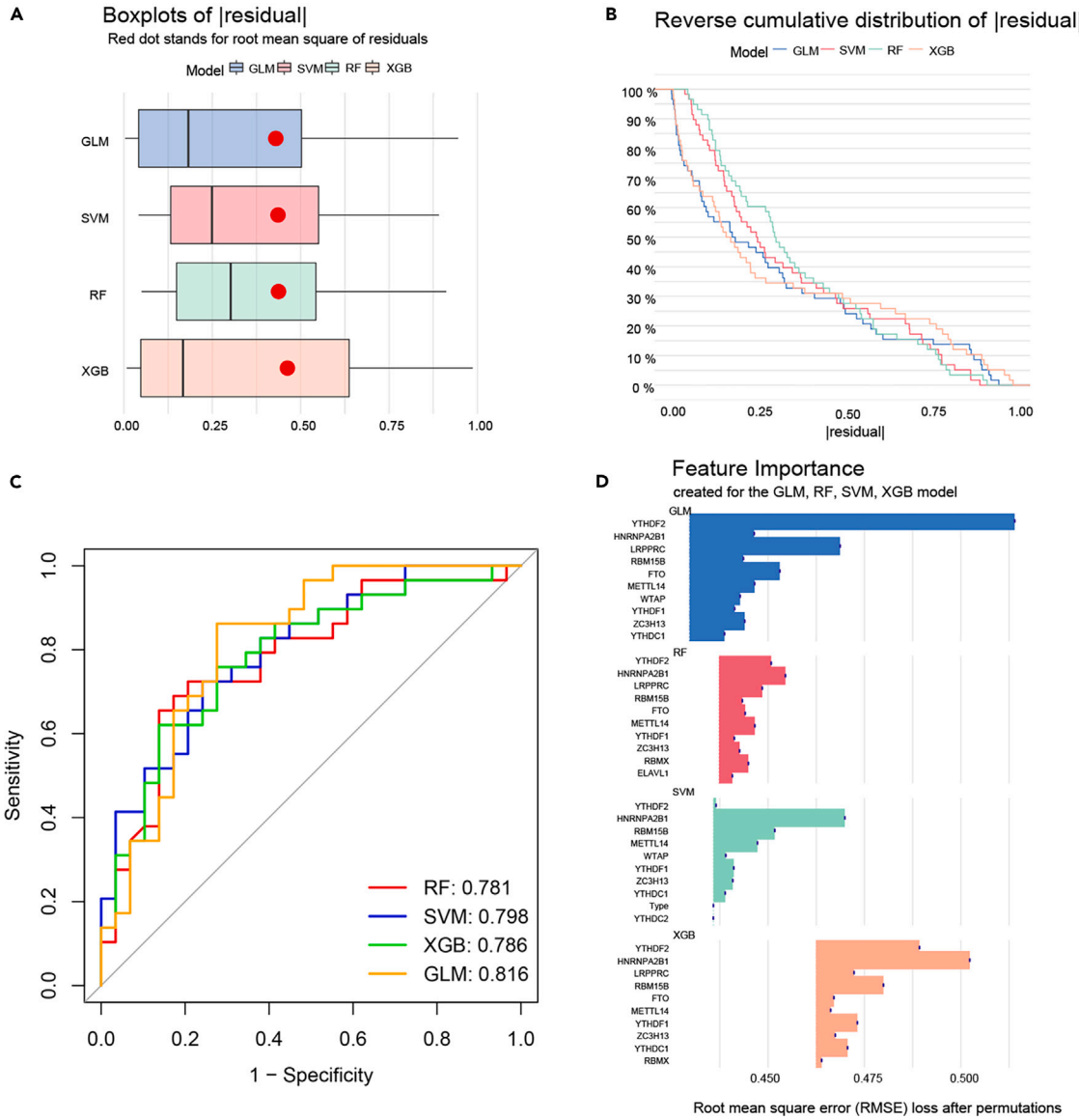

Figure 3. The identification of key genes in AD based on machine learning algorithms

(A) Boxplots of residuals in GLM, SVM, RF, XGB models.

(B) Reverse cumulative distribution of residuals in GLM, SVM, RF, XGB models.

(C) The ROC curves predict the accuracy of each learning machine model.

(D) Top ten key m6A genes in GLM, RF, SVM, and XGB models.

Construction and validation of nomogram model

In order to predict the risk of AD, we used the "rms" package to construct the nomogram model based on the three key genes (YTHDF2, LRPPRC, and FTO, Figure 4A). The calibration curve was a graphical representation of the predictive model's calibration, indicating that the nomogram model exhibited good calibration, with the predicted risk of AD occurrence being consistent with the actual risk (Figure 4B). The decision curve analysis (DCA) curve showed that between the threshold of 0.2–0.8, patients using this model benefited more than those with no intervention or complete intervention (Figure 4C). Based on the DCA curve, we further evaluated the clinical impact curve. In the range of high risk threshold value 0.4–1, the "high risk number" curve was close to the "high risk with event number" curve (Figure 4D), indicating that the nomogram model had strong predictive ability. Finally, we constructed ROC curve based on validation dataset GSE5281 to judge the predictive ability of this model. The area under the ROC curve greater than 0.7 indicates that the model exhibited good discriminative ability and demonstrates good accuracy in predicting AD (Figures 4E and 4F). Therefore, the model demonstrated a certain ability to predict AD.

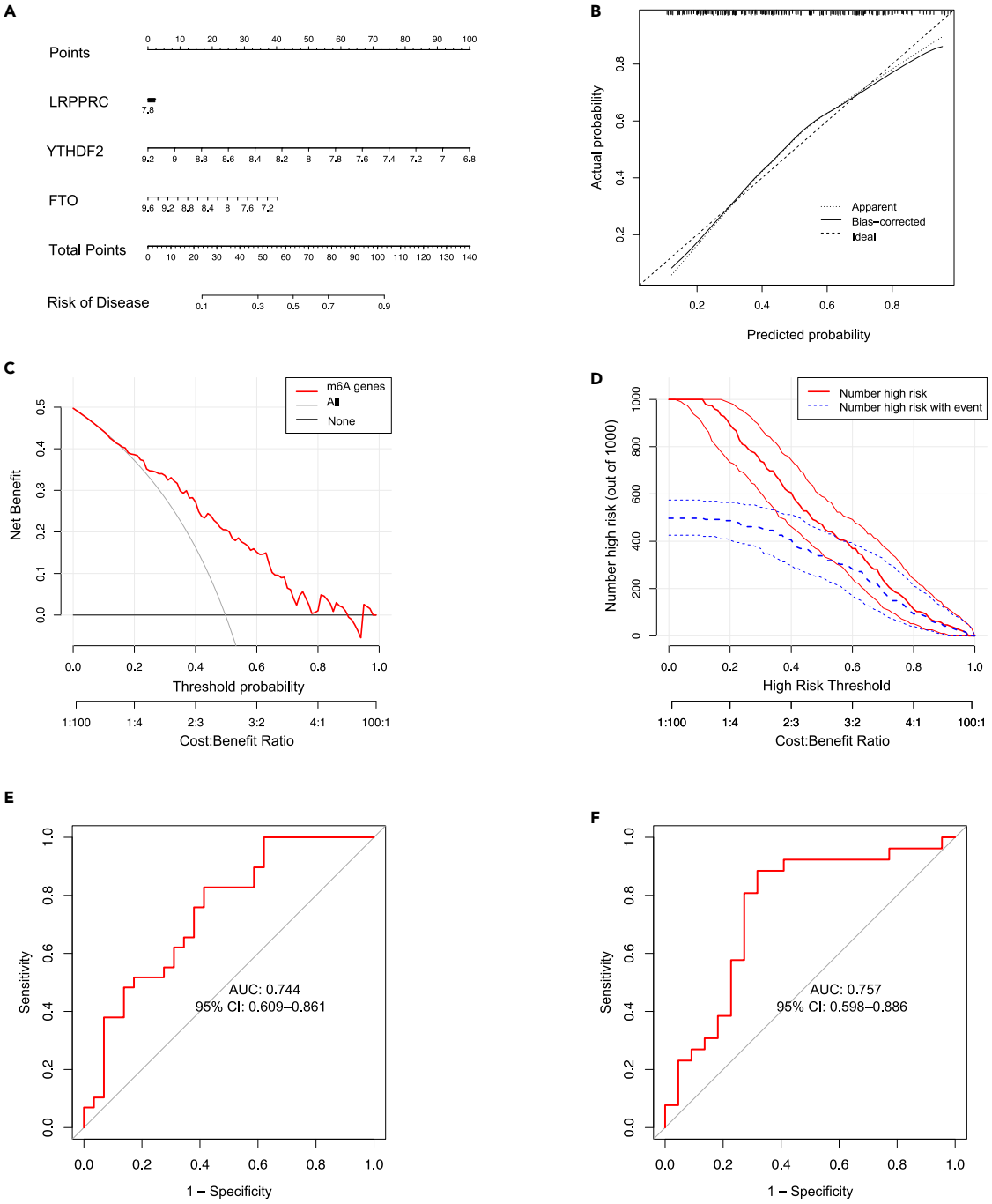

Figure 4. Construction and validation of nomogram model

(A) A nomogram was constructed to predict the prevalence of AD based on three key m6A genes.

(B) The calibration curve showed the predictive accuracy of the nomogram model.

(C) The DCA curve showed the benefits for patients of the nomogram model.

(D) The clinical impact curve showed the clinical impact of the predictive model. (E) The ROC curve showed the predictive accuracy of the nomogram model in the train set.

(F) The ROC curve showed the predictive accuracy of the nomogram model in the validation set.

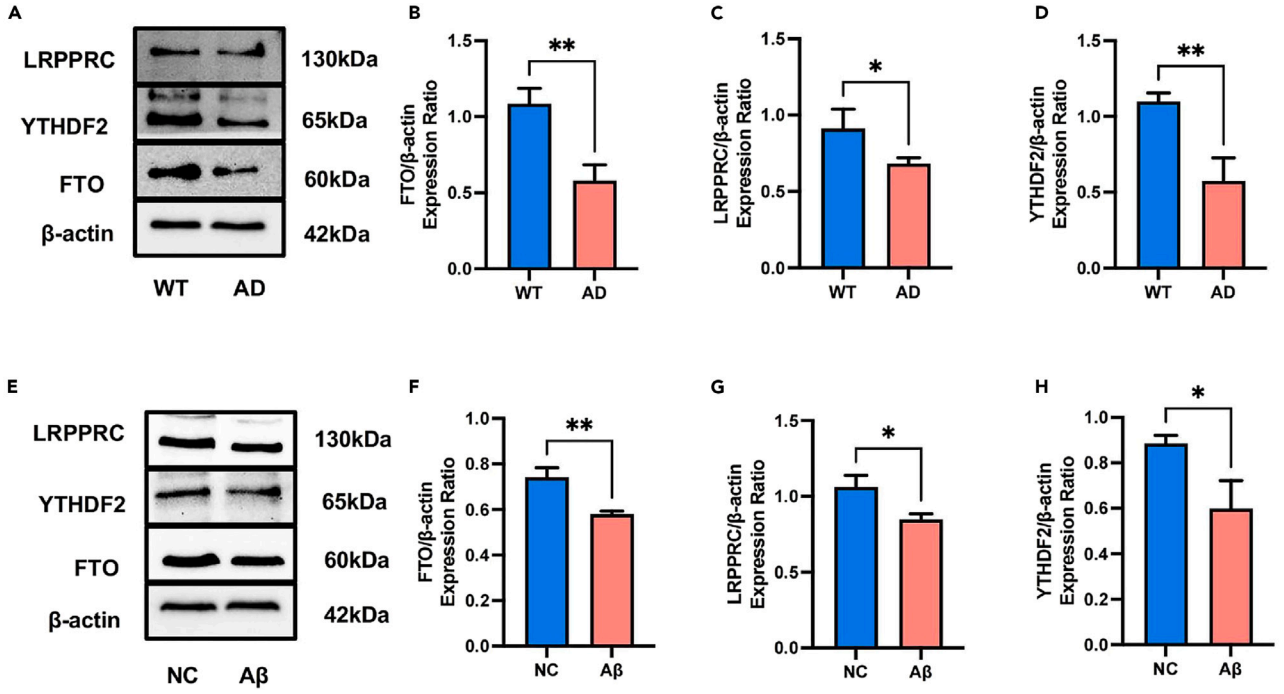

Figure 5. The expression of key m6Aregulators in AD mice model and AD cell model

(A) Representative immunoblots of LRPPRC, YTHDF2, and FTO proteins in the WT group and AD group.

(B–D) Relative abundance of FTO, LRPPRC, and YTHDF2 protein levels in the WT group and AD group.

(E) Representative immunoblots of LRPPRC, YTHDF2, and FTO proteins in the NC group and Aβ group of HT22 cells.

(F–H) Relative abundance of FTO, LRPPRC, and YTHDF2 protein levels in the NC group and Aβ group of HT22 cells. WB: $n = 3$, data were represented as mean ± SEM, $^{*}p < 0.05$, $^{**}p < 0.01$ was considered statistically significant.

The expression of key m6A regulators in AD mice model and AD cell model

Western blot was used to detect the expression of YTHDF2, LRPPRC, and FTO in AD mice and Aβ induced HT22 cells compared to NC. The expression of YTHDF2, LRPPRC, and FTO were decreased in AD mice as well as AD cells compared to control group (Figure 5A–5H, $p < 0.05$, $p < 0.01$). These results validated the three key m6A genes expression patterns in AD.

Immune microenvironment in AD and normal groups

We explored immune infiltration in AD and normal groups via single-sample gene set enrichment analysis (ssGSEA) analysis. The result showed that activated CD8 T cell, CD56dim NK cell, immature B cell, MDSC, mast cell, NK T cell, NK cell, neutrophil, plasmacytoid dendritic cell, and T follicular helper cell were higher enriched in the AD group compared to the normal group (Figure 6A, $p < 0.05$, $p < 0.01$, $p < 0.001$). The overactivation of immune cells such as CD8 T cells and NK cells can not only secrete inflammatory cytokines but also over-activate microglia, thus promoting the progression of Alzheimer's disease.[29,30] However, activated B cell and activated CD4 T cell were lower enriched in the AD group (Figure 6A, $p < 0.05$, $p < 0.01$, $p < 0.001$). It has been reported that B cell depletion in the early stage of Alzheimer's disease promotes Aβ deposition and exacerbates cognitive impairment in AD mice.[31] The loss of CD4 T cells will lead to immature development of brain microglia and affect brain development and immune function.[32] These results indicated that disorders of immune infiltration in the brain may contribute to the progression of Alzheimer's disease.

In addition, the correlation analysis showed that NK cells, MDSC, immature B cells, and dendritic cells which were highly expressed in AD group were negatively associated with key m6A genes, while CD4 T cells were positively associated (Figure 6B). Moreover, we analyzed the differences in the degree of immune cell infiltration between high and low expression of each key gene, and the results were consistent with the correlation analysis (Figurree 6C–6E, $p < 0.05$, $p < 0.01$, $p < 0.001$). It suggested that the decreased expression of m6A may activate the abnormal immune response in AD patients.

Pathway analysis of key m6A genes

We applied a single-gene GSEA analysis to investigate the biological function and pathway of key m6A genes. Notch signaling pathway was negatively associated with FTO, YTHDF2, and LRPPRC. Besides, FTO, YTHDF2, and LRPPRC were positively linked with some cellular functional pathways, such as oxidative phosphorylation and synaptic vesicular circulation (Figure 7A–7F). The dysfunction of Notch signaling has

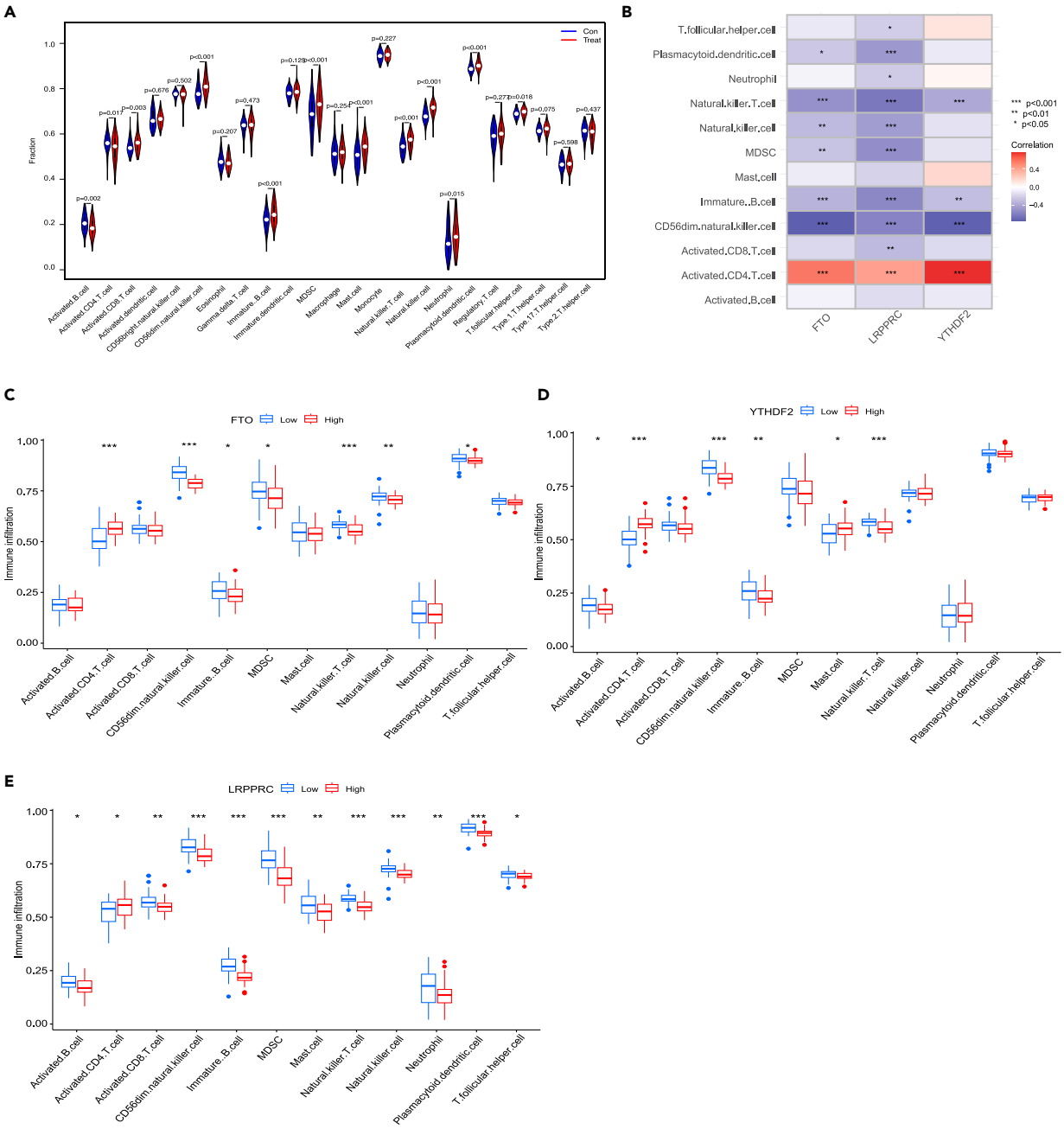

Figure 6. Immune microenvironment in AD and normal groups

(A) The abundance of immune cells in AD and normal groups exhibited in the violin diagram.

(B) The correlation of three key m6A regulators and immune infiltration via Pearson correlation analysis.

(C–E) The infiltration of immune cells in the high and low expression groups of key m6A genes were visualized by boxplots. Data were represented as mean ± SEM. $*p < 0.05$, $**p < 0.01$, $***p < 0.001$ was considered statistically significant.

been reported to play a key role in the pathophysiology of neurodegenerative diseases.[33] These data indicated that key m6A genes might associate with cellular functions and Notch signaling pathway, involving in neurodegeneration diseases.

The exploration of Notch signaling pathway

Notch signaling pathway has been shown to be regulated by m6A genes and plays an important role in cell proliferation, differentiation, apoptosis and other processes.[34] Notch mainly contains Notch1, Notch2, Notch3, and Notch4. We explored the expression of Notch1–4

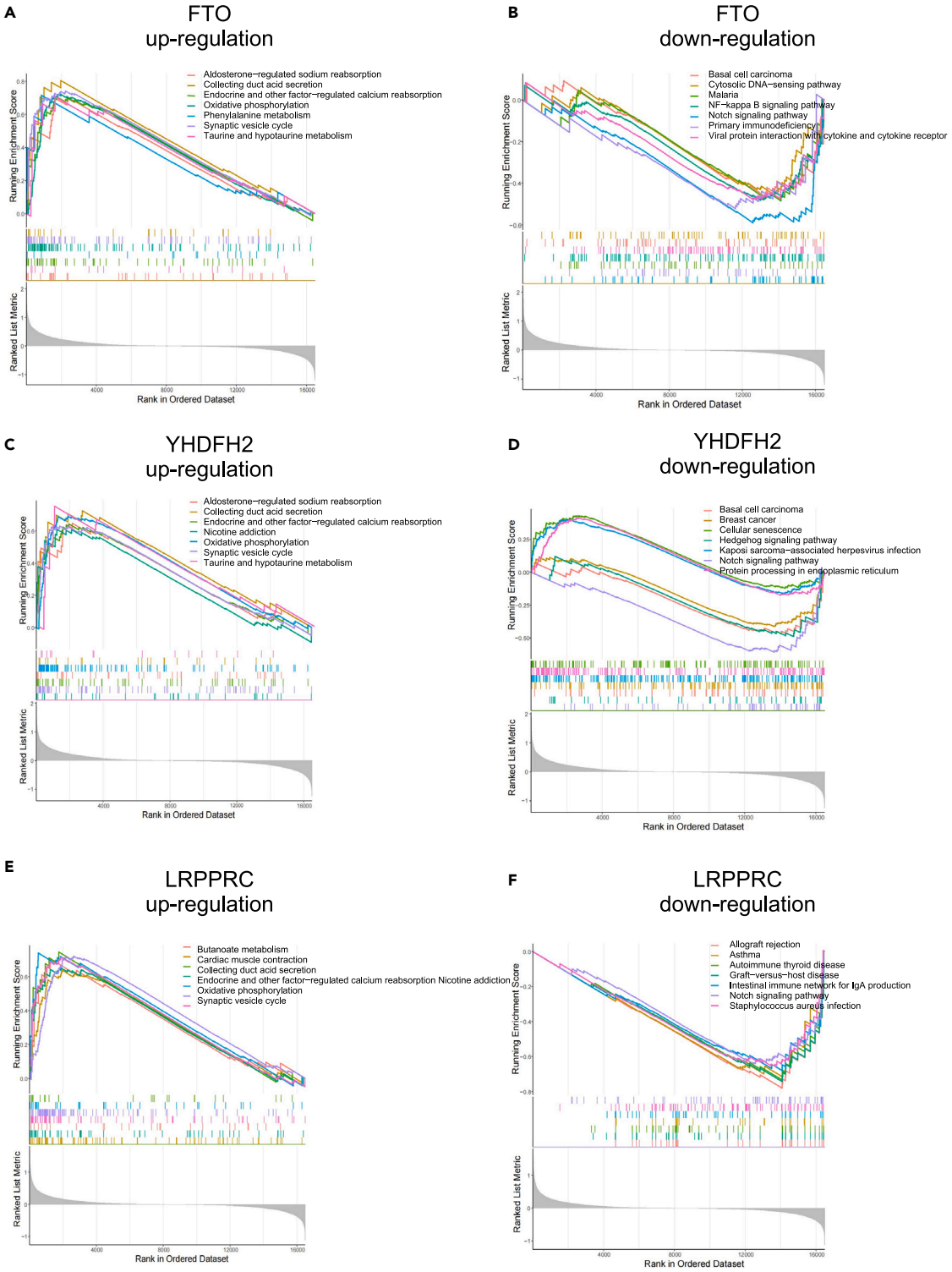

Figure 7. Pathway and function analysis of three key m6A genes

(A, C, and E) Top seven pathways positively associated with FTO, YTHDF2, and LRPPRC.

(B, D, and F) Top seven pathways negatively associated with FTO, YTHDF2, and LRPPRC.

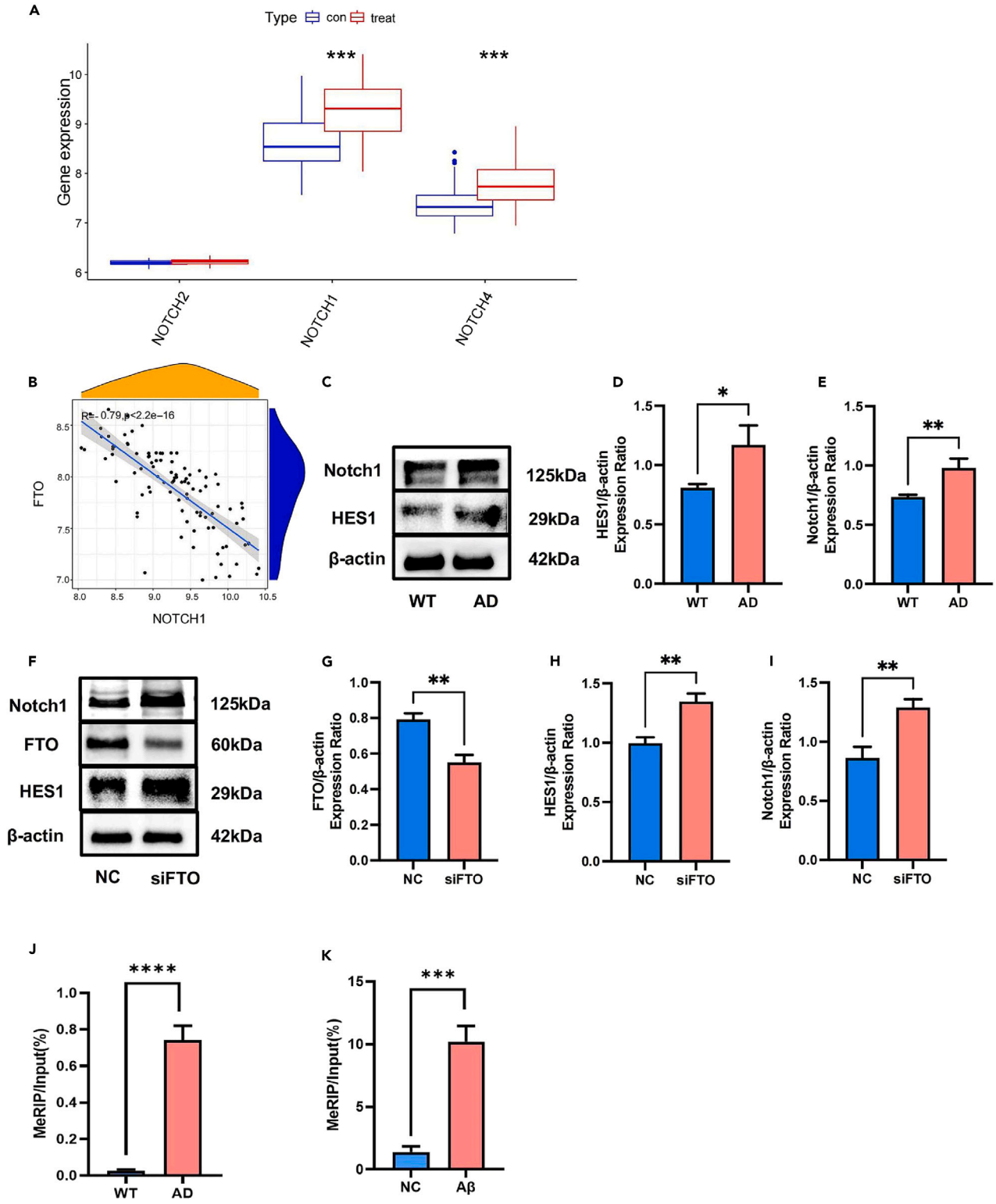

Figure 8. The exploration of Notch signaling pathway

(A) The expression of Notch1, 2, and 4 in normal vs. AD groups exhibited in the boxplot.

(B) The scatter-plot showed the highest correlation between key m6A gene and Notch: FTO and Notch1.

(C) Representative immunoblots of HES1, Notch1, and β-actin proteins in the WT vs. AD.

Figure 8. *Continued*

(D and E) Representative immunoblots of HES1, Notch1, FTO, and β-actin proteins in the NC vs. siFTO of HT22 cells (n = 3).

(F) Relative abundance of HES1 and Notch1 protein levels in the WT vs. AD group.

(G–I) Relative abundance of HES1, Notch1, and FTO protein levels in the NC vs. siFTO of HT22 cells (n = 3).

(J) The levels of m6A methylation of Notch1 mRNA in WT vs. AD group (n = 3).

(K) The levels of m6A methylation of Notch1 mRNA NC vs. Aβ of HT22 cells (n = 3). Data were represented as mean ± SEM. *p < 0.05, **p < 0.01, ***p < 0.001,****p < 0.0001 was considered statistically significant.

in AD and normal groups. The result showed that the expressions of Notch1 and Notch4 were up-regulated in AD group than normal group (Notch3 was not expressed in the dataset) (Figure 8A, $p < 0.001$). Next, the correlation analysis between three key m6A genes and Notch showed that FTO and Notch1 had the greatest correlation (Figure 8B, see also Figure S1-S2). It suggested that FTO might negatively regulate the Notch1 signaling pathway. HES1 is the downstream signal factor of Notch1.[35] Thus, we silenced the expression of FTO in HT22 cells to validate the relationship between FTO and Notch1/HES1 pathway. It showed that the expression of Notch1 and HES1 was significantly increased after silencing the FTO expression in HT22 cells compared to NC group (Figures 8F–8I, $p < 0.01$), indicating that FTO could suppress Notch1 signaling pathway. In addition, western blot was used to detect the expression of Notch1 and HES1 in AD and WT mice. The expression of Notch1 and HES1 was up-regulated in AD mice than WT mice (Figures 8C–8E, $p < 0.05$, $p < 0.01$). We further validated the m6A methylation of Notch1 in both AD mouse model and cell model. In comparison to the control group, there was a significant increase of the Notch1 m6A modification in AD mice and Aβ-treated HT22 cells (Figures 8J and 8K, $p < 0.001$, $p < 0.0001$), contrary to the decrease of FTO. Therefore, the decreased expression of FTO may directly up–regulate the m6A modification of Notch1 mRNA, consequently activating the Notch1/HES1 pathway and contributing to the development of AD.

Exploration of the relationship between m6A, Notch1 pathway, and immune cell

Among immune cells, dendritic cells (DC) are at the forefront of innate immune response and adaptive immune response, which can intensify or inhibit neuroinflammation.[36] Abnormal activation of DC can lead to imbalanced immune response, and even lead to autoimmune reaction and other immunopathology.[37] We performed double immunostaining for the expression of dendritic cell markers CD11c, Notch1, and FTO in the brain regions of AD mice and WT mice to evaluate the link among FTO, Notch1, and immune cells in the brain of mice. We found that compared with WT mice, the brain dendritic cells of AD mice were significantly activated (Figures 9A and 9B, $p < 0.01$), and the Notch1 signal on dendritic cells was significantly up-regulated (Figures 9A and 9D, $p < 0.01$), while FTO level was decreased (Figures 9B and 9E $p < 0.001$). In previous studies, histone deacetylase (HDAC) inhibitor VPA has been shown to up-regulate the expression of Notch1.[38] To further validate the impact of elevated Notch1 signaling on dendritic cell activation, we intervened dendritic cells with VPA at different concentration gradients. As a result, Notch1 expression was up-regulated (Figure 9F, $p < 0.05$, $p < 0.001$) , and with the increase in Notch1 expression, dendritic cells exhibited elevated secretion of inflammatory cytokines tumor necrosis factor-α (TNF-α) and interleukin-1β (IL-1β) (Figures 9G and 9H, $p < 0.01$, $p < 0.001$). It suggested that low expression of FTO may abnormally activate dendritic cells by reducing the inhibition of Notch1 signaling, thereby promoting neuroinflammation and contributing to the progression of Alzheimer's disease.

DISCUSSION

In this study, based on the AD dataset in GEO, we had some interesting findings: (1) The quantified scores of m6A regulators were lower in AD patients than in the normal group. Additionally, m6A RNA methylation was elevated in the AD mice compared to WT mice. (2) Based on differentially expressed m6A genes, three key m6A genes (YTHDF2, LRPPRC, and FTO) were selected by machine learning, and the Norman model constructed by them had good predictive value in which whose downregulation induced AD via immune dysfunction. Meanwhile, the expression pattern of the key three m6A genes was verified in animal and cell AD models. (3) The three key m6A genes might be involved in neurodegenerative diseases by regulating Notch pathway through ssGSEA analysis and among them FTO has the strongest correlation with Notch: it was then demonstrated that in AD cell and animal models, down-regulated FTO activates Notch1/Hes1 signaling pathway. (4)Activation of Notch1 in dendritic cells leads to an increase of the inflammatory cytokines TNF-α and IL-1β *in vitro*. Therefore, the downregulation of m6A genes mainly disturbed the immune microenvironment via FTO-Notch1 signaling pathway, thus promotes the occurrence and development of AD (Figure 10).

Previous studies have reported that the disorder of m6A modification would promote the progression of AD.[18,39] 16 important m6A regulators were screened out through differential expression analysis between AD and normal samples. The expressions of WTAP, CBLL1, YTHDC2, YTHDF2, HNRNPC, LRPPRC, ELAVL1, and FTO were significantly down-regulated in AD samples compared to normal control samples, while METTL14, ZC3H13 RBM15B, YTHDC1 YTHDF1, HNRNP2B1, IGFBP3, and RBMX expressions were up-regulated in the AD group, prompting that the abnormal expression of m6A regulators might link to the development and progression of AD. Additionally, we found that the scores of m6A regulators in AD samples were significantly lower than normal samples. Furthermore, m6A methylation was increased in the hippocampus of AD mice compared to WT mice. Previous studies have demonstrated that several m6A regulators play a key role in the brain by influencing m6A RNA methylation. For instance, YTHDF1 positively regulates m6A modification of the Robo3.1, a member of the Roundabout (Robo) family of axon guidance receptors, participating in axon guidance in the spinal cord. Downregulation of FTO can lead to overall elevation of m6A levels in mice, ultimately inhibiting the proliferation and differentiation of neural progenitor cells.[40] YTHDF2 participates in regulating mouse neural development through its influence on m6A modification of genes related to neural development, and its loss results

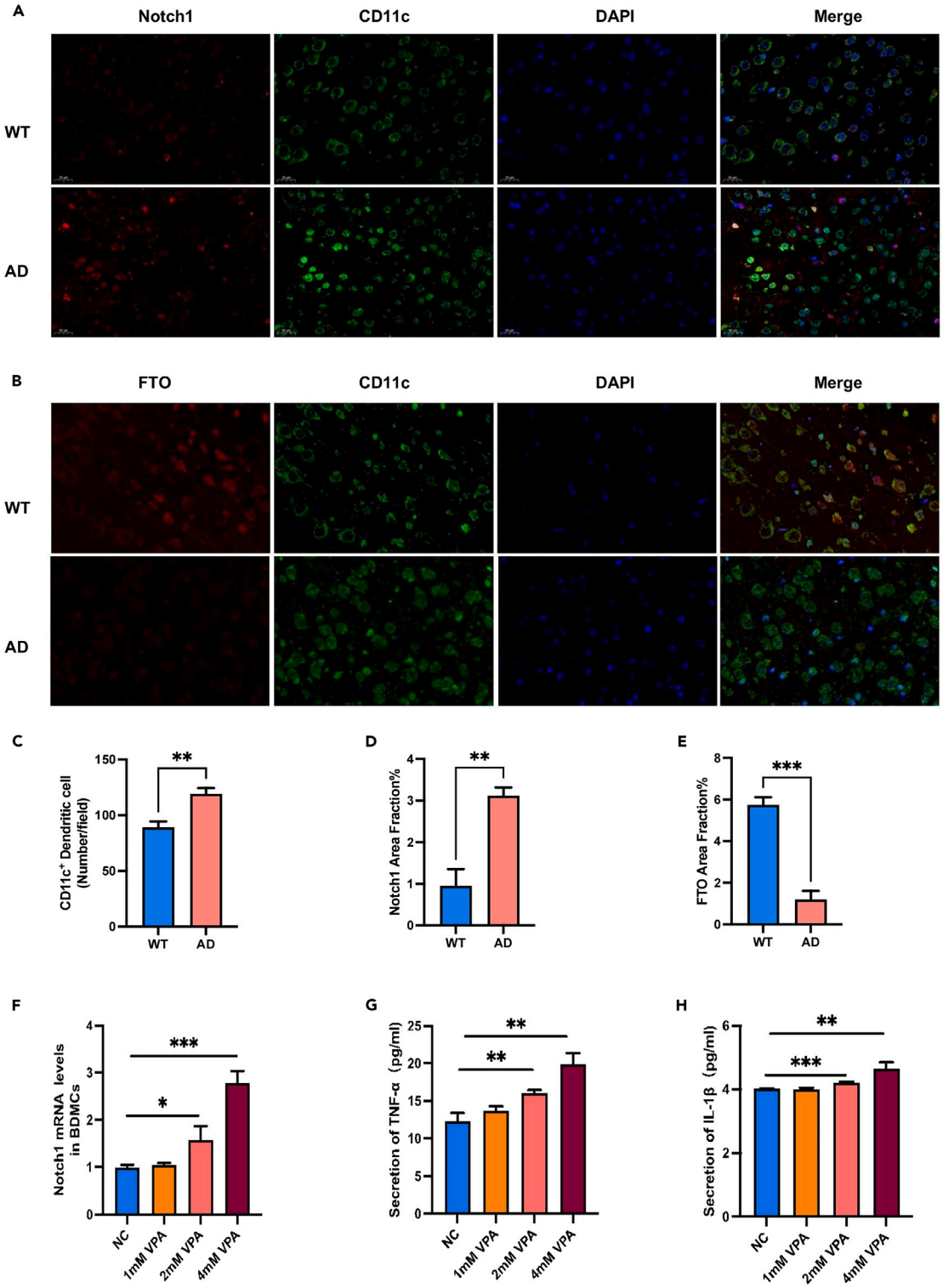

Figure 9. The relationship between FTO, notch1 pathway and dendritic cell

(A) Representative images of Notch1 and CD11c positive immune-fluorescence staining in the brain of WT and AD mice (scale bar: 20 μm). The Notch1 protein (red) is stained with CY3, the dendritic cells markers CD11c (green) is stained with FITC and the nucleus (blue) is stained with DAPI.

(B) Representative images of FTO and CD11c positive immune-fluorescence staining in the brain of WT and AD mice (scale bar: 20 μm). The FTO protein (red) is stained with CY3, the dendritic cells marker CD11c (green) is stained with FITC and the nucleus (blue) is stained with DAPI.

Figure 9. *Continued*

(C) Quantification of $CD11c^+$ dendritic cells in images of AD mice and WT mice.

(D and E) Quantification of Notch1 and FTO positive immune-fluorescence staining in the brain of WT and AD mice ($n = 3$).

(F) The mRNA expression of Notch1 in dendritic cells treated with sodium valproate (VPA) at concentrations of 0, 1 mM, 2 mM, and 4 mM ($n = 3$).

(G and H) The level of TNF-α and IL-1β in culture supernatants of dendritic cells treated with sodium valproate (VPA) at concentrations of 0, 1 mM, 2 mM, and 4 mM ($n = 3$). Data were represented as mean ± SEM, $*p < 0.05$, $**p < 0.01$, $***p < 0.001$ was considered statistically significant.

in abnormal development of the cerebral cortex.[17] These studies suggested that the abnormal expression of m6A genes may lead to neuronal dysplasia, which may ultimately result in the occurrence of AD.

Three key m6A regulators were selected through machine learning algorithms, which were YTHDF2, LRPPRC, and FTO in order of importance. Previous studies have reported that the expression of LRPPRC and FTO in the brain tissues of AD patients and AD mice was significantly decreased[41–43] and may be closely related to the growth and development of neurons. Few studies have been conducted on YTHDF2 in AD. However, YTHDF2 has been reported to be involved in the stages of neuronal development and function.[44] These studies suggested that the three key m6A genes were of great importance in regulating neuron development, which was related to AD.

In the research of AD, commonly used *in vitro* cell models include primary cultured neurons and neural stem cells.[45,46] Recently, clonal cell lines, such as HT22 cells, have gradually become popular in AD studies due to their ease of acquisition and cultivation. The HT22 cell line is an immortalized mouse hippocampal neuron cell line that does not express cholinergic and glutamate receptors like mature hippocampal neurons *in vivo*, which makes it an unsuitable model for memory loss studies of AD.[47] However, it is still widely used for studies on inflammation and oxidative stress signaling pathways involved in AD.[48,49] In some of our experiments, Aβ-induced HT22 cell models and AD mice were used to verify the differences in the expression of three m6A regulators between AD and normal groups.

The expression of YTHDF2, LRPPRC, and FTO was down-regulated in AD mice and Aβ-induced HT22 cells compared to control groups. In addition, the prediction model constructed based on three m6A genes could assess the risk of AD. The calibration curve suggested that the nomogram model had good calibration, with the predicted risk of AD occurrence being consistent with the actual risk. The ROC curve indicated that the model had good discriminative ability, showing excellent accuracy in predicting AD. The clinical impact curve also suggested that the model had strong predictive power, and the DCA curve showed that patients could benefit more with this model. The model demonstrated a certain ability to predict AD, which could contribute to the diagnosis and intervention of AD. These data indicated that the three key m6A regulators might be an important variable of AD development.

Immune response is significantly disturbed in the brains of AD patients. Our study showed that many types of T cells, B cells, NK cells, and dendritic cells were significantly up-regulated in the brains of AD patients. The recruitment of dendritic cells increases significantly in the neuroinflammatory state of the brain, and its precursors can produce inflammatory chemokines to further stimulate T cell response.[50] Similarly, CD8 T cells were enriched in the brain of AD patients, upregulating inflammation signaling.[51] Meanwhile, we found that activated CD4 T cells and B cells were down-regulated in AD samples. As previously mentioned, the loss of CD4 T cells and B cells leads to microglia dysfunction, Aβ deposition, and accelerated progression of Alzheimer's disease.[31,32] These studies showed that abnormal immune responses in the brain might contribute to the progression of Alzheimer's disease. Furthermore, m6A modification plays an important role in immune and inflammatory regulation. For instance, the absence of FTO can lead to the overactivation of NK cells and promote the secretion of interleukin family factors.[52] Similarly, our study found that key m6A genes were negatively associated with NK cells, CD8 T cells, and dendritic cells and positively associated with activated CD4 T cells. These data suggested that the downregulation of key m6A genes might promote abnormal immune response and be involved in the occurrence and development of AD.

Furthermore, ssGSEA analysis was applied to explore the potential functional pathway of three key m6A genes. Three key m6A genes were mainly enriched in Notch signaling pathway and cellular functions. Previous research has shown that m6A genes can negatively regulate Notch signaling.[34,53] The disorder of Notch signaling pathway may accelerate the progress of AD.[33,54] It indicated that low expression of m6A genes might activate Notch signaling pathway and thus aggravate the progression of AD.

Notch mainly contains Notch1 to Notch4. We found that the expression of Notch1 and Notch4 was higher in AD group than normal group. Besides, our study showed that Notch1 and Notch4 were negatively associated with three key m6A regulators, specially FTO had the strongest association with Notch1. In order to validate the relationship between FTO and Notch1 pathway, we silenced FTO expression in HT22 cells, showing that Notch1 signaling pathway was up-regulated. Subsequently, we validated the m6A methylation of Notch1 mRNA in both AD mouse model and cell model. In comparison to the control group, there was a significant increase in the m6A methylation of Notch1 mRNA in AD mice and Aβ-treated HT22 cells. This increase was contrary to the reduced expression of FTO. Therefore, FTO may directly exert negative regulation on the Notch1 m6A modification, subsequently modulating the Notch1 signaling pathway negatively. Previous studies have shown conflicting results regarding the impact of Notch1 m6A modification on Notch1 signaling. In non-small cell lung cancer models, Notch1 m6A modification has been demonstrated to reduce the stability of Notch1 mRNA, leading to decreased Notch1 expression.[55] However, other research supports that Notch1 m6A modification can enhance Notch1 expression, thereby upregulating the Notch1 signaling pathway.[56] The specific mechanism awaits further investigation.

Activation of Notch1 signaling pathway can promote the activation of brain immune cells and up-regulate the release of tumor necrosis factor, interleukin-6, and other inflammatory factors.[57] Our result showed that dendritic cells were activated in AD mice and Notch1 expression was up-regulated in dendritic cells, while FTO level was down-regulated. Besides, upregulating the expression of Notch1 in dendritic cells leads to an increase of the inflammatory cytokines TNF-α and IL-1β *in vitro*. These data suggested that downregulation of FTO expression leads to decreased inhibition of Notch1 signaling, which activates the brain immune response. Overactivation of immune cells can cause

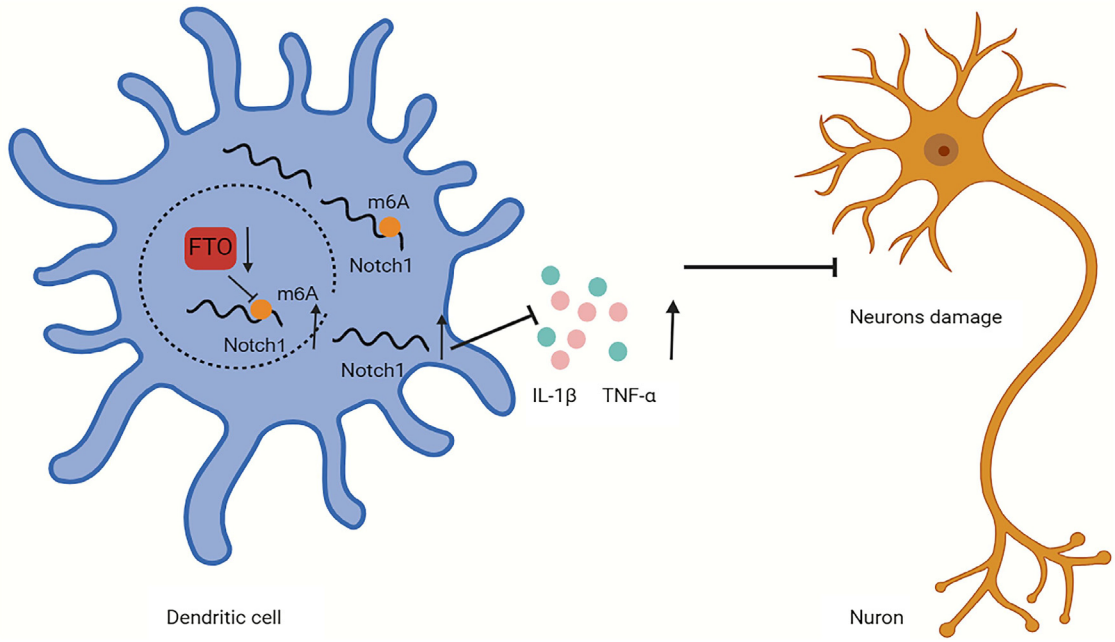

Figure 10. The relationship between m6A and immune cells

Proposed mechanism may be that abnormally low expression of m6A genes in the brain reduces the inhibition of Notch1 m6A modification and Notch1 signaling on immune cells, overactivation of immune cells leads to increased secretion of pro-inflammatory factors, damage to neurons, and promote the progression of Alzheimer's disease.

cell death in multiple ways, thus promoting the release of inflammatory factors, leading to chronic nerve inflammation, promoting Tau protein hyperphosphorylation and Aβ deposition, thus promoting the progression of Alzheimer's disease[58]

Overall, downregulation of FTO may lead to disruption of the brain's immune microenvironment and contribute to the progression of Alzheimer's disease via upregulating the m6A modification of Notch1 mRNA and Notch1-HES1 activation. Moreover, three m6A regulators (YTHDF2, LRPPRC, and FTO) might be new targets for immune regulation of Alzheimer's disease but need further investigation for their overall and singular effects.

Conclusion

Our study suggested that three key m6A regulators (YTHDF2, LRPPRC, and FTO) were candidates as potential biomarkers for AD, and models constructed from these three key m6A regulators predicted the risk of AD. The most important regulator in the model is FTO, whose down-regulation might promote the progression of AD by activation of immune response via Notch1-HES1 pathway.

Limitations of the study

In this study, we investigated the crucial m6A regulator FTO and its influence on the progression of Alzheimer's disease through the Notch1-HES1 pathway. However, due to financial and technical constraints, we were unable to directly down-regulate FTO in animal models to further validate this pathway. Additionally, we did not assess the m6A RNA methylation in AD patients, nor did we measure the levels of FTO and Notch1-HES1. Furthermore, the precise mechanisms of action of the other two m6A regulators, YTHDF2 and LRPPRC, in the progression of Alzheimer's disease necessitate further comprehensive investigation.

STAR★METHODS

Detailed methods are provided in the online version of this paper and include the following:

- KEY RESOURCES TABLE
- RESOURCE AVAILABILITY
  - Lead contact
  - Materials availability
  - Data and code availability
- EXPERIMENTAL MODEL AND STUDY PARTICIPANT DETAILS
  - Animals and cells

SUPPLEMENTAL INFORMATION

Supplemental information can be found online at https://doi.org/10.1016/j.isci.2024.110235.

ACKNOWLEDGMENTS

This study was supported by National Science Foundation of China (Project # 82270861 to Dr. Gao), the Fundamental Research Funds for the Central Universities (Project # 2042020kf1079 to Dr. Gao), the Planned international development Project of Wuhan University.

AUTHOR CONTRIBUTIONS

Y.M., D.L., and L.G. conceptualized the study; Y.Q. and Y.M. performed experiments; Y.Q., Y.M., and M.X. performed statistical analysis; Y.Q., Y.M., and L.G. prepared the manuscript.

DECLARATION OF INTERESTS

The authors declare no competing interests.

Received: June 26, 2023
Revised: March 17, 2024
Accepted: May 19, 2024
Published: June 8, 2024

REFERENCES

1. Josephine Boder, E., and Banerjee, I.A. (2021). Alzheimer's Disease: Current Perspectives and Advances in Physiological Modeling. Bioengineering (Basel) *8*, 211. https://doi.org/10.3390/bioengineering8120211.
2. Knobel, P., Litke, R., and Mobbs, C.V. (2022). Biological age and environmental risk factors for dementia and stroke: Molecular mechanisms. Front. Aging Neurosci. *14*, 1042488. https://doi.org/10.3389/fnagi.2022.1042488.
3. Giallongo, S., Longhitano, L., Denaro, S., D'Aprile, S., Torrisi, F., La Spina, E., Giallongo, C., Mannino, G., Lo Furno, D., Zappalà, A., et al. (2022). The Role of Epigenetics in Neuroinflammatory-Driven Diseases. Int. J. Mol. Sci. *23*, 15218. https://doi.org/10.3390/ijms232315218.
4. Gao, X., Chen, Q., Yao, H., Tan, J., Liu, Z., Zhou, Y., and Zou, Z. (2022). Epigenetics in Alzheimer's Disease. Front. Aging Neurosci. *14*, 911635. https://doi.org/10.3389/fnagi.2022.911635.
5. Chouliaras, L., Mastroeni, D., Delvaux, E., Grover, A., Kenis, G., Hof, P.R., Steinbusch, H.W.M., Coleman, P.D., Rutten, B.P.F., and van den Hove, D.L.A. (2013). Consistent decrease in global DNA methylation and hydroxymethylation in the hippocampus of Alzheimer's disease patients. Neurobiol. Aging *34*, 2091–2099. https://doi.org/10.1016/j.neurobiolaging.2013.02.021.
6. Tang, Y., Chen, K., Song, B., Ma, J., Wu, X., Xu, Q., Wei, Z., Su, J., Liu, G., Rong, R., et al. (2021). m6A-Atlas: a comprehensive knowledgebase for unraveling the N6-methyladenosine (m6A) epitranscriptome. Nucleic Acids Res. *49*, D134–D143. https://doi.org/10.1093/nar/gkaa692.
7. Roundtree, I.A., Evans, M.E., Pan, T., and He, C. (2017). Dynamic RNA Modifications in Gene Expression Regulation. Cell *169*, 1187–1200. https://doi.org/10.1016/j.cell.2017.05.045.
8. Wang, X., Lu, Z., Gomez, A., Hon, G.C., Yue, Y., Han, D., Fu, Y., Parisien, M., Dai, Q., Jia, G., et al. (2014). N6-methyladenosine-dependent regulation of messenger RNA stability. Nature *505*, 117–120. https://doi.org/10.1038/nature12730.
9. Luo, Q., Mo, J., Chen, H., Hu, Z., Wang, B., Wu, J., Liang, Z., Xie, W., Du, K., Peng, M., et al. (2022). Structural insights into molecular mechanism for N(6)-adenosine methylation by MT-A70 family methyltransferase METTL4.

Nat. Commun. *13*, 5636. https://doi.org/10.1038/s41467-022-33277-x.

10. Pupak, A., Singh, A., Sancho-Balsells, A., Alcalá-Vida, R., Espina, M., Giralt, A., Martí, E., Ørom, U.A.V., Ginés, S., and Brito, V. (2022). Altered m6A RNA methylation contributes to hippocampal memory deficits in Huntington's disease mice. Cell. Mol. Life Sci. *79*, 416. https://doi.org/10.1007/s00018-022-04444-6.
11. Liu, H., Lyu, H., Jiang, G., Chen, D., Ruan, S., Liu, S., Zhou, L., Yang, M., Zeng, S., He, Z., et al. (2022). ALKBH5-mediated m6A demethylation of GLUT4 mRNA promotes glycolysis and resistance to HER2-targeted therapy in breast cancer. Cancer Res. *82*, 3974–3986. https://doi.org/10.1158/0008-5472.CAN-22-0800.
12. Ruffenach, G., Medzikovic, L., Aryan, L., Li, M., and Eghbali, M. (2022). HNRNPA2B1: RNA-Binding Protein That Orchestrates Smooth Muscle Cell Phenotype in Pulmonary Arterial Hypertension. Circulation *146*, 1243–1258. https://doi.org/10.1161/CIRCULATIONAHA.122.059591.
13. Arguello, A.E., DeLiberto, A.N., and Kleiner, R.E. (2017). RNA Chemical Proteomics Reveals the N(6)-Methyladenosine (m(6)A)-Regulated Protein-RNA Interactome. J. Am. Chem. Soc. *139*, 17249–17252. https://doi.org/10.1021/jacs.7b09213.
14. Liu, W., Liu, C., You, J., Chen, Z., Qian, C., Lin, W., Yu, L., Ye, L., Zhao, L., and Zhou, R. (2022). Pan-cancer analysis identifies YTHDF2 as an immunotherapeutic and prognostic biomarker. Front. Cell Dev. Biol. *10*, 954214. https://doi.org/10.3389/fcell.2022.954214.
15. Livneh, I., Moshitch-Moshkovitz, S., Amariglio, N., Rechavi, G., and Dominissini, D. (2020). The m(6)A epitranscriptome: transcriptome plasticity in brain development and function. Nat. Rev. Neurosci. *21*, 36–51. https://doi.org/10.1038/s41583-019-0244-z.
16. Wang, C.X., Cui, G.S., Liu, X., Xu, K., Wang, M., Zhang, X.X., Jiang, L.Y., Li, A., Yang, Y., Lai, W.Y., et al. (2018). METTL3-mediated m6A modification is required for cerebellar development. PLoS Biol. *16*, e2004880. https://doi.org/10.1371/journal.pbio.2004880.
17. Li, M., Zhao, X., Wang, W., Shi, H., Pan, Q., Lu, Z., Perez, S.P., Suganthan, R., He, C., Bjørås, M., and Klungland, A. (2018). Ythdf2-mediated m(6)A mRNA clearance modulates neural development in mice. Genome Biol. *19*, 69. https://doi.org/10.1186/s13059-018-1436-y.
18. Shafik, A.M., Zhang, F., Guo, Z., Dai, Q., Pajdzik, K., Li, Y., Kang, Y., Yao, B., Wu, H., He, C., et al. (2021). N6-methyladenosine dynamics in neurodevelopment and aging, and its potential role in Alzheimer's disease. Genome Biol. *22*, 17. https://doi.org/10.1186/s13059-020-02249-z.
19. Wang, Y., Li, L., Li, J., Zhao, B., Huang, G., Li, X., Xie, Z., and Zhou, Z. (2021). The Emerging Role of m6A Modification in Regulating the Immune System and Autoimmune Diseases. Front. Cell Dev. Biol. *9*, 755691. https://doi.org/10.3389/fcell.2021.755691.
20. Mapperley, C., van de Lagemaat, L.N., Lawson, H., Tavosanis, A., Paris, J., Campos, J., Wotherspoon, D., Durko, J., Sarapuu, A., Choe, J., et al. (2021). The mRNA m6A reader YTHDF2 suppresses proinflammatory pathways and sustains hematopoietic stem cell function. J. Exp. Med. *218*, e20200829. https://doi.org/10.1084/jem.20200829.
21. Burgaletto, C., Munafò, A., Di Benedetto, G., De Francisci, C., Caraci, F., Di Mauro, R., Bucolo, C., Bernardini, R., and Cantarella, G. (2020). The immune system on the TRAIL of Alzheimer's disease. J. Neuroinflammation *17*, 298. https://doi.org/10.1186/s12974-020-01968-1.
22. Chen, Y., and Colonna, M. (2022). Spontaneous and induced adaptive immune responses in Alzheimer's disease: new insights into old observations. Curr. Opin. Immunol. *77*, 102233. https://doi.org/10.1016/j.coi.2022.102233.
23. Jevtic, S., Sengar, A.S., Salter, M.W., and McLaurin, J. (2017). The role of the immune system in Alzheimer disease: Etiology and treatment. Ageing Res. Rev. *40*, 84–94. https://doi.org/10.1016/j.arr.2017.08.005.
24. Li, J., Zhang, Y., Lu, T., Liang, R., Wu, Z., Liu, M., Qin, L., Chen, H., Yan, X., Deng, S., et al. (2022). Identification of diagnostic genes for both Alzheimer's disease and Metabolic syndrome by the machine learning algorithm. Front. Immunol. *13*, 1037318. https://doi.org/10.3389/fimmu.2022.1037318.
25. Shiino, A., Shirakashi, Y., Ishida, M., and Tanigaki, K.; Japanese Alzheimer's Disease Neuroimaging Initiative (2021). Machine learning of brain structural biomarkers for Alzheimer's disease (AD) diagnosis, prediction of disease progression, and amyloid beta deposition in the Japanese population. Alzheimers Dement. *13*, e12246. https://doi.org/10.1002/dad2.12246.
26. Hayes, M.R., Borner, T., and De Jonghe, B.C. (2021). The Role of GIP in the Regulation of GLP-1 Satiety and Nausea. Diabetes *70*, 1956–1961. https://doi.org/10.2337/dbi21-0004.
27. Zhao, Y., Che, Y., Liu, Q., Zhou, S., and Xiao, Y. (2023). Analyses of m6A regulatory genes and subtype classification in atrial fibrillation. Front. Cell. Neurosci. *17*, 1073538. https://doi.org/10.3389/fncel.2023.1073538.
28. Zhang, H., Meltzer, P., and Davis, S. (2013). RCircos: an R package for Circos 2D track plots. BMC Bioinf. *14*, 244. https://doi.org/10.1186/1471-2105-14-244.
29. Unger, M.S., Li, E., Scharnagl, L., Poupardin, R., Altendorfer, B., Mrowetz, H., Hutter-Paier, B., Weiger, T.M., Heneka, M.T., Attems, J., and Aigner, L. (2020). CD8(+) T-cells infiltrate Alzheimer's disease brains and regulate neuronal- and synapse-related gene expression in APP-PS1 transgenic mice. Brain Behav. Immun. *89*, 67–86. https://doi.org/10.1016/j.bbi.2020.05.070.
30. Qi, C., Liu, F., Zhang, W., Han, Y., Zhang, N., Liu, Q., and Li, H. (2022). Alzheimer's disease alters the transcriptomic profile of natural killer cells at single-cell resolution. Front. Immunol. *13*, 1004885. https://doi.org/10.3389/fimmu.2022.1004885.
31. Xiong, L.L., Xue, L.L., Du, R.L., Niu, R.Z., Chen, L., Chen, J., Hu, Q., Tan, Y.X., Shang, H.F., Liu, J., et al. (2021). Single-cell RNA sequencing reveals B cell-related molecular biomarkers for Alzheimer's disease. Exp. Mol. Med. *53*, 1888–1901. https://doi.org/10.1038/s12276-021-00714-8.
32. Pasciuto, E., Burton, O.T., Roca, C.P., Lagou, V., Rajan, W.D., Theys, T., Mancuso, R., Tito, R.Y., Kouser, L., Callaerts-Vegh, Z., et al. (2020). Microglia Require CD4 T Cells to Complete the Fetal-to-Adult Transition. Cell *182*, 625–640.e24. https://doi.org/10.1016/j.cell.2020.06.026.
33. Kapoor, A., and Nation, D.A. (2021). Role of Notch signaling in neurovascular aging and Alzheimer's disease. Semin. Cell Dev. Biol. *116*, 90–97. https://doi.org/10.1016/j.semcdb.2020.12.011.
34. Lee, B., Lee, S., and Shim, J. (2021). YTHDF2 Suppresses Notch Signaling through Post-transcriptional Regulation on Notch1. Int. J. Biol. Sci. *17*, 3776–3785. https://doi.org/10.7150/ijbs.61573.
35. Jin, Z., Guo, P., Li, X., Ke, J., Wang, Y., and Wu, H. (2019). Neuroprotective effects of irisin against cerebral ischemia/reperfusion injury via Notch signaling pathway. Biomed. Pharmacother. *120*, 109452. https://doi.org/10.1016/j.biopha.2019.109452.
36. Constant, O., Maarifi, G., Blanchet, F.P., Van de Perre, P., Simonin, Y., and Salinas, S. (2022). Role of Dendritic Cells in Viral Brain Infections. Front. Immunol. *13*, 862053. https://doi.org/10.3389/fimmu.2022.862053.
37. Liu, J., Zhang, X., Cheng, Y., and Cao, X. (2021). Dendritic cell migration in inflammation and immunity. Cell. Mol. Immunol. *18*, 2461–2471. https://doi.org/10.1038/s41423-021-00726-4.
38. Greenblatt, D.Y., Cayo, M.A., Adler, J.T., Ning, L., Haymart, M.R., Kunnimalaiyaan, M., and Chen, H. (2008). Valproic acid activates Notch1 signaling and induces apoptosis in medullary thyroid cancer cells. Ann. Surg. *247*, 1036–1040. https://doi.org/10.1097/SLA.0b013e3181758d0e.
39. Zhao, F., Xu, Y., Gao, S., Qin, L., Austria, Q., Siedlak, S.L., Pajdzik, K., Dai, Q., He, C., Wang, W., et al. (2021). METTL3-dependent RNA m(6)A dysregulation contributes to neurodegeneration in Alzheimer's disease through aberrant cell cycle events. Mol. Neurodegener. *16*, 70. https://doi.org/10.1186/s13024-021-00484-x.
40. Li, L., Zang, L., Zhang, F., Chen, J., Shen, H., Shu, L., Liang, F., Feng, C., Chen, D., Tao, H., et al. (2017). Fat mass and obesity-associated (FTO) protein regulates adult neurogenesis. Hum. Mol. Genet. *26*, 2398–2411. https://doi.org/10.1093/hmg/ddx128.
41. Bennett, J.P., Jr., and Keeney, P.M. (2020). Alzheimer's and Parkinson's brain tissues have reduced expression of genes for mtDNA OXPHOS Proteins, mitobiogenesis regulator PGC-1α protein and mtRNA stabilizing protein LRPPRC (LRP130). Mitochondrion *53*, 154–157. https://doi.org/10.1016/j.mito.2020.05.012.
42. Shen, L., Yang, A., Chen, X., Xiao, S., Liu, X., Lin, J., Zhao, Y., Zhang, K., Li, C., Ke, J., et al. (2022). Proteomic Profiling of Cerebrum Mitochondria, Myelin Sheath, and Synaptosome Revealed Mitochondrial Damage and Synaptic Impairments in Association with 3 × Tg-AD Mice Model. Cell. Mol. Neurobiol. *42*, 1745–1763. https://doi.org/10.1007/s10571-021-01052-z.
43. Han, M., Liu, Z., Xu, Y., Liu, X., Wang, D., Li, F., Wang, Y., and Bi, J. (2020). Abnormality of m6A mRNA Methylation Is Involved in Alzheimer's Disease. Front. Neurosci. *14*, 98. https://doi.org/10.3389/fnins.2020.00098.
44. Kumar, S., Tsai, L.W., Kumar, P., Dubey, R., Gupta, D., Singh, A.K., Swarup, V., and Singh, H.N. (2021). Genome-Wide Scanning of Potential Hotspots for Adenosine Methylation: A Potential Path to Neuronal Development. Life *11*, 1185. https://doi.org/10.3390/life11111185.
45. Radio, N.M., and Mundy, W.R. (2008). Developmental neurotoxicity testing in vitro: models for assessing chemical effects on neurite outgrowth. Neurotoxicology *29*,

361–376. https://doi.org/10.1016/j.neuro.2008.02.011.

46. Li, X., Bao, X., and Wang, R. (2016). Experimental models of Alzheimer's disease for deciphering the pathogenesis and therapeutic screening (Review). Int. J. Mol. Med. *37*, 271–283. https://doi.org/10.3892/ijmm.2015.2428.
47. He, M., Liu, J., Cheng, S., Xing, Y., and Suo, W.Z. (2013). Differentiation renders susceptibility to excitotoxicity in HT22 neurons. Neural Regen. Res. *8*, 1297–1306. https://doi.org/10.3969/j.issn.1673-5374.2013.14.006.
48. Zhao, Z.Y., Luan, P., Huang, S.X., Xiao, S.H., Zhao, J., Zhang, B., Gu, B.B., Pi, R.B., and Liu, J. (2013). Edaravone protects HT22 neurons from H2O2-induced apoptosis by inhibiting the MAPK signaling pathway. CNS Neurosci. Ther. *19*, 163–169. https://doi.org/10.1111/cns.12044.
49. Ji, Y.J., Kim, S., Kim, J.J., Jang, G.Y., Moon, M., and Kim, H.D. (2021). Crude Saponin from Platycodon grandiflorum Attenuates Aβ-Induced Neurotoxicity via Antioxidant, Anti-Inflammatory and Anti-Apoptotic Signaling Pathways. Antioxidants *10*, 1968. https://doi.org/10.3390/antiox10121968.
50. Worbs, T., Hammerschmidt, S.I., and Förster, R. (2017). Dendritic cell migration in health and disease. Nat. Rev. Immunol. *17*, 30–48. https://doi.org/10.1038/nri.2016.116.
51. Altendorfer, B., Unger, M.S., Poupardin, R., Hoog, A., Asslaber, D., Gratz, I.K., Mrowetz, H., Benedetti, A., de Sousa, D.M.B., Greil, R., et al. (2022). Transcriptomic Profiling Identifies CD8(+) T Cells in the Brain of Aged and Alzheimer's Disease Transgenic Mice as Tissue-Resident Memory T Cells. J. Immunol. *209*, 1272–1285. https://doi.org/10.4049/jimmunol.2100737.
52. Kim, S.M., Oh, S.C., Lee, S.Y., Kong, L.Z., Lee, J.H., and Kim, T.D. (2023). FTO negatively regulates the cytotoxic activity of natural killer cells. EMBO Rep. *24*, e55681. https://doi.org/10.15252/embr.202255681.
53. Gu, C., Wang, Z., Zhou, N., Li, G., Kou, Y., Luo, Y., Wang, Y., Yang, J., and Tian, F. (2019). Mettl14 inhibits bladder TIC self-renewal and bladder tumorigenesis through N(6)-methyladenosine of Notch1. Mol. Cancer *18*, 168. https://doi.org/10.1186/s12943-019-1084-1.
54. Perna, A., Marathe, S., Dreos, R., Falquet, L., Akarsu Egger, H., and Auber, L.A. (2021). Revealing NOTCH-dependencies in synaptic targets associated with Alzheimer's disease. Mol. Cell. Neurosci. *115*, 103657. https://doi.org/10.1016/j.mcn.2021.103657.
55. Shen, Y., Li, C., Zhou, L., and Huang, J.A. (2021). G protein-coupled oestrogen receptor promotes cell growth of non-small cell lung cancer cells via YAP1/QKI/circNOTCH1/m6A methylated NOTCH1 signalling. J. Cell Mol. Med. *25*, 284–296. https://doi.org/10.1111/jcmm.15997.
56. Chohan, H., Senkevich, K., Patel, R.K., Bestwick, J.P., Jacobs, B.M., Bandres Ciga, S., Gan-Or, Z., and Noyce, A.J. (2021). Type 2 Diabetes as a Determinant of Parkinson's Disease Risk and Progression. Mov. Disord. *36*, 1420–1429. https://doi.org/10.1002/mds.28551.
57. Cheng, M., Yang, L., Dong, Z., Wang, M., Sun, Y., Liu, H., Wang, X., Sai, N., Huang, G., and Zhang, X. (2019). Folic acid deficiency enhanced microglial immune response via the Notch1/nuclear factor kappa B p65 pathway in hippocampus following rat brain I/R injury and BV2 cells. J. Cell Mol. Med. *23*, 4795–4807. https://doi.org/10.1111/jcmm.14368.
58. Rajesh, Y., and Kanneganti, T.D. (2022). Innate Immune Cell Death in Neuroinflammation and Alzheimer's Disease. Cells *11*, 1885. https://doi.org/10.3390/cells11121885.
59. Guo, R., Dai, J., Xu, H., Zang, S., Zhang, L., Ma, N., Zhang, X., Zhao, L., Luo, H., Liu, D., and Zhang, J. (2022). The diagnostic significance of integrating m6A modification and immune microenvironment features based on bioinformatic investigation in aortic dissection. Front. Cardiovasc. Med. *9*, 948002. https://doi.org/10.3389/fcvm.2022.948002.
60. Wu, H., Feng, J., Wu, J., Zhong, W., Zouxu, X., Huang, W., Huang, X., Yi, J., and Wang, X. (2023). Prognostic value of comprehensive typing based on m6A and gene cluster in TNBC. J. Cancer Res. Clin. Oncol. *149*, 4367–4380. https://doi.org/10.1007/s00432-022-04345-y.
61. Sun, M., Xie, M., Zhang, T., Wang, Y., Huang, W., and Xia, L. (2021). m(6)A Methylation Modification Patterns and Tumor Microenvironment Infiltration Characterization in Pancreatic Cancer. Front. Immunol. *12*, 739768. https://doi.org/10.3389/fimmu.2021.739768.
62. Pan, X., Jin, X., Wang, J., Hu, Q., and Dai, B. (2021). Placenta inflammation is closely associated with gestational diabetes mellitus. Am. J. Transl. Res. *13*, 4068–4079.
63. Hou, N., Li, M., He, L., Xie, B., Wang, L., Zhang, R., Yu, Y., Sun, X., Pan, Z., and Wang, K. (2020). Predicting 30-days mortality for MIMIC-III patients with sepsis-3: a machine learning approach using XGboost. J. Transl. Med. *18*, 462. https://doi.org/10.1186/s12967-020-02620-5.
64. Xu, D., Wang, Y., Liu, X., Zhou, K., Wu, J., Chen, J., Chen, C., Chen, L., and Zheng, J. (2021). Development and clinical validation of a novel 9-gene prognostic model based on multi-omics in pancreatic adenocarcinoma. Pharmacol. Res. *164*, 105370. https://doi.org/10.1016/j.phrs.2020.105370.
65. Zheng, J., Xie, Y., Ren, L., Qi, L., Wu, L., Pan, X., Zhou, J., Chen, Z., and Liu, L. (2021). GLP-1 improves the supportive ability of astrocytes to neurons by promoting aerobic glycolysis in Alzheimer's disease. Mol. Metab. *47*, 101180. https://doi.org/10.1016/j.molmet.2021.101180.
66. Lutz, M.B., Kukutsch, N., Ogilvie, A.L., Rössner, S., Koch, F., Romani, N., and Schuler, G. (1999). An advanced culture method for generating large quantities of highly pure dendritic cells from mouse bone marrow. J. Immunol. Methods *223*, 77–92. https://doi.org/10.1016/s0022-1759(98)00204-x.
67. Mei, Y., Li, Y., Cheng, Y., and Gao, L. (2023). The effect of gastric bypass surgery on cognitive function of Alzheimer's disease and the role of GLP1-SGLT1 pathway. Exp. Neurol. *363*, 114377. https://doi.org/10.1016/j.expneurol.2023.114377.
68. Zhang, L., Zhou, Y., Yang, L., Wang, Y., and Xiao, Z. (2023). PACAP6-38 improves nitroglycerin-induced central sensitization by modulating synaptic plasticity at the trigeminal nucleus caudalis in a male rat model of chronic migraine. J. Headache Pain *24*, 66. https://doi.org/10.1186/s10194-023-01603-3.

STAR★METHODS

KEY RESOURCES TABLE

REAGENT or RESOURCE	SOURCE	IDENTIFIER
Antibodies		
Anti-FTO	Abclonal	Cat# A20992;RRID: AB_3105769
Anti-LRPPRC	Abclonal	Cat# A3365;RRID: AB_2765075
Anti-YTHDF2	Abclonal	Cat# A15616;RRID: AB_2763022
Anti-Notch1	Abclonal	Cat# A19090;RRID: AB_2862582
Anti-Notch1	Abclonal	Cat# A7636;RRID: AB_2863555
Anti-HES1	Abclonal	Cat# A0925;RRID: AB_2861486
Anti-CD11c	Abcam	Cat# ab23602;RRID: AB_2129794
Anti-β-actin	Abclonal	Cat# AC038;RRID: AB_2863784
Chemicals, peptides, and recombinant proteins		
$A\beta_{1-42}$ peptide	Maokangbio	MP5401
Sodium valproate	MCE	HY10585A
LPS	Sigma	L4391
IL-4	PeproTech	214-14
rmGM-CSF	PeproTech	315-03
Critical commercial assays		
m6A RNA Methylation Quantification Kit	A&D Technology Corporation	A-P-9005
rioboMeRIP™ m6A Transcriptome Profiling Kit	RioboBo	C11051-1
SweScript All-in-One RT SuperMix for qPCR kit	Servicebio	G3337-50
Universal Blue SYBR Green qPCR Master Mix	Servicebio	G3326-01
Mouse Tumor Necrosis Factor Alpha (TNF-a) ELISA Kit	Jianglai Biosciences	JL10484
Mouse Interleukin 1 Beta (IL-1β) ELISA Kit	Jianglai Biosciences	JL18442
Experimental models: Cell lines		
HT22	Wuhan Pinuo Fei Co	N/A
Bone marrow-derived dendritic cells	C57BL/6J mice	N/A
Experimental models: Organisms		
APP/PS1/Tau triple transgenic mice	Jackson Laboratory	N/A
C57BL/6J mice	China Three Gorges University	N/A
Oligonucleotides		
See Tables S2 and S3	RiboBio, Servicebio	N/A
Software and algorithms		
R-4.2.1	R project	N/A
GraphPad Prism 8.0.1	GraphPad	N/A

RESOURCE AVAILABILITY

Lead contact

Further information and requests for resources and reagents should be directed to and will be fulfilled by the lead contact, Ling Gao (ling.gao@whu.edu.cn).

Materials availability

This study did not generate new unique reagents.

Data and code availability

- All data reported in this paper will be shared by the lead contact upon request.
- This paper did not report original code.
- Any additional information required to reanalyze the data reported in this paper is available from the lead contact upon request.

EXPERIMENTAL MODEL AND STUDY PARTICIPANT DETAILS

Animals and cells

Male APP/PS1/Tau triple transgenic mice (AD mice) were purchased from Jackson Laboratory. Male C57BL/6J mice (WT mice) were purchased from China Three Gorges University. The hippocampal tissues were harvested at ten months of age for subsequent analysis. Mouse hippocampal neuron cell line HT22 was purchased from Wuhan Pinuo Fei Co., LTD. Bone marrow-derived dendritic cells (BMDCs) were obtained from male C57BL/6J mice (6–8 weeks). All animal experiments were approved by the Experimental Center of Renmin Hospital of Wuhan University (20210904A).

METHOD DETAILS

Data acquisition

The GSE132903 dataset (97 AD vs. 98 control) was downloaded from the Gene Expression Omnibus database, which was sequenced via GPL10558 platform. The gene expression profile was normalized by the "normalizeBetweenArrays" function in the "limma" package of R software (4.2.1). In addition, GSE5281 was downloaded as an external validation dataset (87 AD vs. 74 control), which was obtained by GLP570 platform. The basic characters of two datasets were listed in Table S1. Meanwhile, twenty-three m6A genes were obtained from previous studies.[59,60]

Protein-protein interaction network

Twenty-three m6A regulators was constructed as a protein-protein interaction (PPI) network via using STRING, showing the association among m6A genes (interaction score > 0.15).

The exploration of m6A expression pattern

Twenty-three m6A regulators included six m6A writers (METTL3, METTL14, WTAP, ZC3H13, RBM15B, CBLL1); two m6A erasers (ALKBH5 and FTO), and fifteen m6A readers (YTHDC1, YTHDC2, YTHDF1, YTHDF2, YTHDF3, HNRNPC, FMR1, LRPPRC, HNRNPA2B1, IGFBP1, IGFBP2, IGFBP3, RBMX, ELAVL1, IGF2BP1). The expression of m6A genes in AD group and normal group was visualized by a boxplot. The "limma" package was used to obtain differentially expressed m6A genes ($p < 0.05$). Besides, Pearson correlation analysis was applied for the correlation among 16 differentially expressed m6A genes.

Calculation of m6A score via PCA analysis

In order to quantify the m6A modification of each sample, principal component analysis (PCA) was applied to calculate the m6A score of each sample and construct a scoring system to evaluate the m6A modification.[61] It has the advantage of reducing the complexity of the data and identifying the most important gene modules.

$$m6Ascore = \sum(PC\,1i + PC\,2i)$$

where i is the expression of differentially expressed m6A regulators.

Key m6A genes were screened by machine learning algorithm

In order to screen out key m6A genes that contribute significantly to the development of AD, we established four machine learning models, including generalized linear model (GLM), support vector machine model (SVM), random forest model (RF) and XGboost (XGB) model.[62,63] The "DALEX" package [60] in R was used to analyze the four models. A receiver operating characteristic (ROC) curve and the residual distribution was carried out to obtain the optimal model. Finally, three optimal explanatory variables (YTHDF2, LRPPRC, FTO) were selected from the optimal model as key genes.

Construction of a nomogram model

Based on the three key genes screened out by machine learning, we applied the "rms"[64] package to construct a Nomogram model in order to predict the risk of AD patients. The calibration curve was used to determine how well our predicted values match reality. A decision curve analysis (DCA) was performed to assess whether model-based decisions were beneficial to patients. The "pROC" package was used for ROC curve to judge the accuracy of the model. Finally, GSE5281 was used as an external verification set for verification.

Analysis of immune microenvironment in AD and normal groups

Single-sample gene-set enrichment analysis (ssGSEA) was performed using the "GSVA" package to assess immune cell abundance in AD and normal group samples. The expression of immune cells in AD and normal groups was visualized by box diagram. Pearson correlation analysis was applied for the correlation between key m6A genes and immune infiltration. Besides, boxplots were used to visualize the infiltration of immune cells in the high and low expression groups of key m6A genes.

Pathway analysis of key m6A genes

To explore the regulatory pathways and biological functions associated with key m6A genes, single-gene GSEA analysis was performed. The adjusted p value <0.05 was considered be significant. The up-regulated and down-regulated pathways with the top seven enrichment scores were shown respectively.

The exploration of notch signaling pathway

The expression of Notch1-Notch4 in AD and normal groups was visualized by box diagram. The "limma" package was used to obtain differentially expressed Notch genes ($p < 0.05$). Besides, Pearson correlation analysis was applied for the correlation among key m6Agenes and differentially expressed Notch genes.

Cell culture and cell transfection

HT22 cells were cultured in high glucose DMEM containing 10% fetal bovine serum and 1% antibiotics in an incubator at 37° C and 5% carbon dioxide. The medium should be changed every two days. FTO siRNA was purchased from RiboBio (Guangzhou, China). The sequence was listed in Table S2. Before cell transfection, HT22 cells were transferred into the six-well plate. When cell density reached about 80%, FTO siRNA and transfection reagent were mixed and added into the six-well plate for 48h.

Aβ treated in HT22 cells

We established an *in vitro* model of Alzheimer's disease by intervening with Aβ in HT22 cells.[49] Before intervention, the cells were placed to six-well plates to reaching 80–90% confluence. $A\beta_{1\text{-}42}$ peptide (Maokangbio) was dissolved in dimethyl sulfoxide and then diluted to a 400uM/ml solution with PBS, which was oligomeric at 4°C for 24 h.[65] HT22 cells were treated with 5uM Aβ each well for 24h in serum-free medium.

Bone marrow-derived dendritic cells and treated with sodium valproate

Bone marrow-derived dendritic cells (BMDCs) were obtained from C57BL/6J mice, as previously described.[66] After extraction, BMDCs were cultured in six-well plates using RPMI 1640 medium (Gibco, USA) supplemented with 10 ng/mL rmGM-CSF and 10 ng/mL IL-4 (PeproTech, America), with media changes every two days. On the 7th day, maturation was induced using 1 μg/mL lipopolysaccharide (LPS) (Sigma, America). On the 9th day, BMDCs were treated with sodium valproate (VPA) (MCE, America) at concentrations of 0 mM, 1 mM, 2 mM, and 4 mM for 48 h. After the intervention, cells and culture supernatants were collected.

Quantification of the m6A modification

First, total RNA was extracted from the hippocampus of AD mice and WT mice. According to the manufacturer's instructions, m6A was quantitatively analyzed using the m6A RNA Methylation Quantification Kit (colorimetric method, A&D Technology Corporation, China). A total of 200 ng of RNA was added to each measurement well, and absorbance at a wavelength of 450 nm was recorded. Subsequently, m6A quantification was performed based on standard curve calculations.

MeRIP-qPCR

We utilized the rioboMeRIP™ m6A Transcriptome Profiling Kit (RioboBo, China) to validate the changes in m6A methylation levels of Notch1 in the mouse hippocampus and HT22 cells. Initially, total RNA was extracted from the hippocampus of WT and AD mice, as well as from Aβ--treated and blank control groups of HT22 cells. Subsequently, the RNA was fragmented into fragments of 100–150 bp in size. These fragments were then immunoprecipitated with magnetic beads containing 5 μg of anti-m6A antibody. After washing and elution, the co-precipitated RNA was separated and used as RNA samples for subsequent RT-qPCR. The primer sequences were listed in Table S3.

Quantitative real-time PCR

Total RNA from dendritic cells was extracted using Trizol reagent. cDNA synthesis was performed using the SweScript All-in-One RT SuperMix for qPCR kit (Servicebio, China). Subsequently, RT-qPCR was conducted using Universal Blue SYBR Green qPCR Master Mix (Servicebio, China) on a LightCycler 480 system (Roche, Germany). GAPDH served as the internal control, and the quantification of mRNA relative expression was conducted using the $2^{-\Delta\Delta Ct}$ method. The primer sequences were listed in Table S3.

Western blotting

The protein extracts were obtained by homogenization and centrifugation of mouse hippocampal tissues and HT22 cells and the specific experimental process was conducted according to our previous work.[67] The primary antibodies contained FTO, LRPPRC, YTHDF2, Notch1, HES1 and β-actin (Abclonal, A20992, A3365, A15616, A19090, A0925). We employed β-actin as an internal reference, and the grayscale values of the bands were analyzed for protein expression levels using ImageJ.

ELISA

After completion of VPA intervention, cell culture supernatants were collected. The levels of TNF-α and IL-1β were quantified following the procedures outlined in the ELISA kit (Jianglai Biosciences, China).

Immunofluorescence staining

Mouse brain tissue was fixed with 4% paraformaldehyde solution and cut into coronal paraffin-embedded tissue sections. The specific experimental process was conducted according to previous work.[68] Primary antibodies contains FTO (1:200) (Abclonal, A20992), Notch1(1:200) (Abclonal, A7636) and CD11c (1:200) (Abcam, ab23602) The percentage of Notch1 and FTO expression and the number of dendritic cells under 400 microscopes was quantified by Image J software.

QUANTIFICATION AND STATISTICAL ANALYSIS

Most statistical analysis was based on R software (4.2.1) and GraphPad Prism (8.0.1). The t-test and one-way analysis of variance (ANOVA) was used to compare the expression of there key m6A genes and Notch-related genes in mice and cell models. $P < 0.05$ was considered statistical significance.